Thermal conductivity of silicon nitride membranes is not sensitive to stress

Hossein Ftouni, Christophe Blanc, Dimitri Tainoff, Andrew D. Fefferman, Martial Defoort, Kunal J. Lulla, Jacques Richard, Eddy Collin, and Olivier Bourgeois*

Institut NÉEL, CNRS, 25 avenue des Martyrs, F-38042 Grenoble, France
and Université Grenoble Alpes, Institut NEEL, F-38042 Grenoble, France

(Received 27 January 2015; published 28 September 2015)

We have measured the thermal properties of suspended membranes from 10 to 300 K for two amplitudes of internal stress (about 0.1 and 1 GPa) and for two different thicknesses (50 and 100 nm). The use of the original 3ω-Volklein method has allowed the extraction of both the specific heat and the thermal conductivity of each SiN membrane over a wide temperature range. The mechanical properties of the same substrates have been measured at helium temperatures using nanomechanical techniques. Our measurements show that the thermal transport in freestanding SiN membranes is not affected by the presence of internal stress. Consistently, mechanical dissipation is also unaffected even though Q's increase with increasing tensile stress. We thus demonstrate that the theory developed by Wu and Yu [J. Wu and C. C. Yu, Phys. Rev. B **84**, 174109 (2011)] does not apply to this amorphous material in this stress range. On the other hand, our results can be viewed as a natural consequence of the "dissipation dilution" argument [Y. L. Huang and P. R. Saulson, Rev. Sci. Instrum. **69**, 544 (1998)], which has been introduced in the context of mechanical damping.

DOI: 10.1103/PhysRevB.92.125439 PACS number(s): 65.60.+a, 68.65.−k, 62.40.+i, 63.50.Lm

I. INTRODUCTION

Silicon nitride (SiN) thin films are widely used to thermally isolate sensitive thermal detectors for etch masking as well as layers for microelectromechanical systems [1]. Indeed, outstanding mechanical properties including very high-quality factors Q [2,3] can be reached in an optimized SiN material. Depending on deposition parameters, SiN films can experience very large residual (biaxial) stress during deposition. It is thus of prime importance to understand the role of the internal stress not only on the mechanical properties but also on the other physical characteristics of SiN films, including optical, thermal, and electrical properties. Silicon nitride has a specific place due to its amorphous nature and the study of stress in that compound is also an issue for the fundamental understanding of its role in the physics of glasses [2].

Use of the stress to tune the thermal properties of nanomaterials is one of the possible ways to design future thermal components (thermal rectifier, thermal diode, thermal switch, etc. [4]). This has been proposed for monocrystalline silicon [5,6], as strain in silicon is currently used to enhance electron mobility in transistors [7]. Since the debate on the origin of mechanical dissipation in strained glasses such as SiN [2,8], the question of the effect of stress on the thermal properties, whatever its origin (internal or external), has been raised and theoretically addressed for the case of silicon nitride [9]. Indeed, it is well known that stoichiometric silicon nitride (Si_3N_4) prepared by low-pressure chemical-vapor deposition (LPCVD) contains a significant internal tensile stress (up to about 1 GPa) as compared to regular nonstoichiometric SiN that has a very low internal stress (below 0.2 GPa). In an attempt to explain the very high mechanical Q's, Wu and Yu [9] proposed a model where the internal losses in the material are sensitive to the stress state. Their calculations based on this hypothesis predict that the thermal conductivity of SiN may be strongly enhanced by the presence of stress. On the other hand, systematic mechanical measurements on high-stress SiN substrates explain the Q's through the so-called dissipation dilution model [10]: mechanical energy is stored through the tensioning of the substrate, while the dissipation is unaffected [9,11,12]. However, no experiments to date have directly compared similar devices made of different SiN materials. Furthermore, thermal properties of low-stress SiN have been widely measured over a broad temperature range [13–18] for different kinds of thin films and nanomaterials, but very few experimental studies deal with the influence of stress on the thermal transport at the nanoscale [19].

In order to study the potential effect of internal stress on the thermal properties of silicon nitride, the thermal conductivity and the specific heat have been measured as a function of temperature for high-stress (HS) and low-stress (LS) SiN membranes having a thickness of 50 and 100 nm. These measurements are performed using the 3ω-Völklein method [20–22] as described in previous papers. This technique allows the measurement of both thermal conductivity and specific heat of a given membrane within the same experiment over a broad temperature range. The mechanical dissipation and stress amplitude of both HS and LS substrates are also measured at cryogenic temperatures by means of nanomechanical resonators [23]. We show experimentally that thermal conduction is essentially independent of the stress stored in this material. This is inconsistent with the hypothesis underlying the model of Ref. [9] for SiN, and corroborates the dissipation dilution explanation for high mechanical Q's.

II. SAMPLES AND EXPERIMENTAL METHODS

The thermal properties of two types of SiN membranes have been measured: high-stress stoichiometric Si_3N_4 and low-stress SiN deposited by LPCVD. The amorphous stoichiometric high-stress (HS) Si_3N_4 as well as low-stress (LS) SiN were grown on both sides of a silicon substrate. The membranes were then patterned on the rear side by laser

*olivier.bourgeois@neel.cnrs.fr

 ©2015 American Physical Society

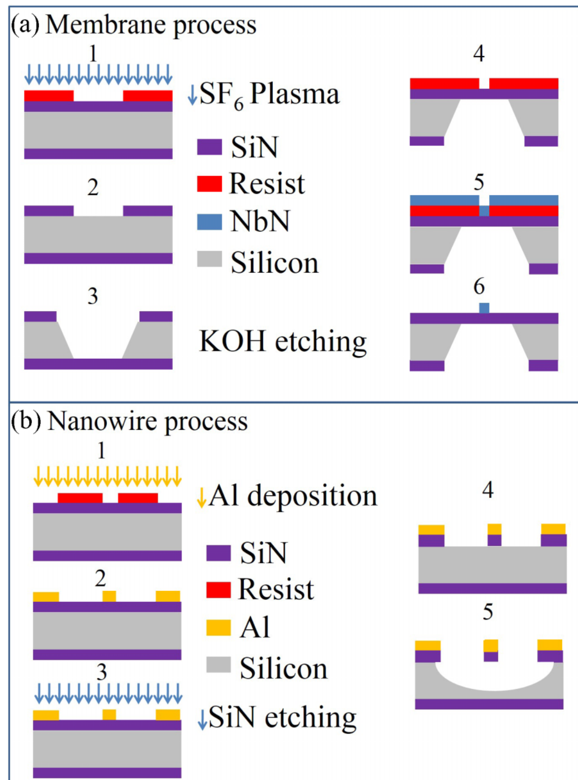

FIG. 1. (Color online) Micro- and nanofabrication processes of both suspended structures studied in this work. (a) Fabrication process for the membranes. For membranes 1 and 2, the patterns of the membranes are created by photolithography. The nonprotected SiN is removed by SF_6 RIE etching. For membrane 3, the silicon is anisotropically etched in a KOH solution. For membrane 4, the thermometers are obtained by a lift-off process; the area is patterned by photolithography. For membrane 5, NbN (70 nm) is deposited by reactive sputtering. For membrane 6, the resist and NbN layer is removed using a wet procedure. (b) Fabrication process for the nanowires. For membrane 1, the patterns of the nanowires are created by electron-beam lithography. For membrane 2, there is evaporation of the Al layer (30 nm). For membranes 3 and 4, the nonprotected SiN is removed by SF_6 RIE. And for membrane 5, the silicon is isotropically etched by gaseous XeF_2 etching.

photolithography. After removing the silicon nitride by SF_6 reactive ion etching (RIE), the silicon substrate on the rear side was etched in potassium hydroxide (KOH), as described in Fig. 1. The final result is a rectangular SiN membrane obtained on the front side.

Before the thermal study, a mechanical measurement was performed to quantify the stress present after releasing the membranes. A suspended silicon nitride beam with 100 nm thickness, 250 nm width, and 15 μm length fabricated using electron-beam lithography from the same substrate was placed in a magnetic field (see Fig. 1 for fabrication details). A sinusoidal driving current within a 30 nm thin deposited Al layer is used to generate the Lorentz force causing the beam's out-of-plane oscillation [24]. This measurement is performed in a vacuum of about 10^{-6} mbar at helium temperatures. The magnetic flux cut by the beam oscillation generates a voltage, which is measured using a lock-in amplifier [3,25]. Typical resonance curves for the first flexure and their respective fits are shown in Fig. 2.

The expression for the nth-mode resonance frequency of a stressed doubly clamped beam is given by [8]

$$f_n = \frac{n}{2}\sqrt{\frac{\sigma}{\rho h^2}}. \tag{1}$$

Equation (1) is used to calculate the stress σ within the beam, with n the mode number, ρ the silicon nitride density ($3\ \mathrm{g/cm^3}$), and h the beam length [23]. We find a stress value of about 0.85 GPa for the HS silicon nitride, which confirms that the membrane is still stressed after releasing, and 0.12 GPa for the LS silicon nitride. These values agree fairly well with the manufacturer data (supplied by LioniX), as they should. Note that both values fall in the high-stress limit of beam theory, validating the use of Eq. (1).

A careful characterization of the setup and devices has been performed in order to guarantee quantitative analysis [25,26]. In particular, the loading from the environment onto the measured resonance has been characterized as a function of magnetic field [24]: the raw resonance lines displayed in Fig. 2 are only about 20% broader than the genuine intrinsic mechanical resonances. The varying shapes and stress of many devices have been measured [26], studying flexural modes up to $n = 9$.

The important and still unsolved issue of the mechanical dissipation shall be discussed elsewhere [27]. But let us nonetheless position our findings within the state of the art. The mechanical Q factors obtained for our high-stress samples are consistent with the literature [8,11,28–30], as are the low-stress results [8,31]. Obviously, these comparisons have to be taken with care, since temperature and metallic coatings are known to influence mechanical dissipation [32–34], but the dispersion among silicon nitride wafer providers seems to be greater than or of the same order as these effects. Comparing very different types of devices had led to the proposition that stress could strongly influence mechanical dissipation [2]. Recent results from Refs. [11,12,28] on HS devices contradict this idea and favor the dissipation dilution model first introduced in Ref. [10]: the mechanical Q factor increases only because the stored (tensioning) energy increases. Indeed, tuning the stress by bending the sample, a linear relationship between Q and f_0 is found in Ref. [8]. In this respect, Fig. 2 is a natural consequence of the dissipation dilution idea: while the mechanical $Q = f_0/\Delta f$ increases with stress, the linewidth Δf (measuring mechanical dissipation) of the resonances of two geometrically identical devices is almost unaffected. The related question we thus want to address in this paper is how stress affects the thermal properties of silicon nitride structures.

Thermal experiments are conducted on the very same materials. As mentioned above, we have chosen in this study the most appropriate method to measure the thermal conductivity of large aspect ratio suspended membranes: the 3ω-Völklein method [20–22]. The principle of the method consists of creating a sinusoidal Joule heating generated by an ac electrical current at frequency ω across a transducer centered along the long axis of a rectangular membrane. The center of the membrane is thermally isolated from the frame and hence its temperature is free to increase.

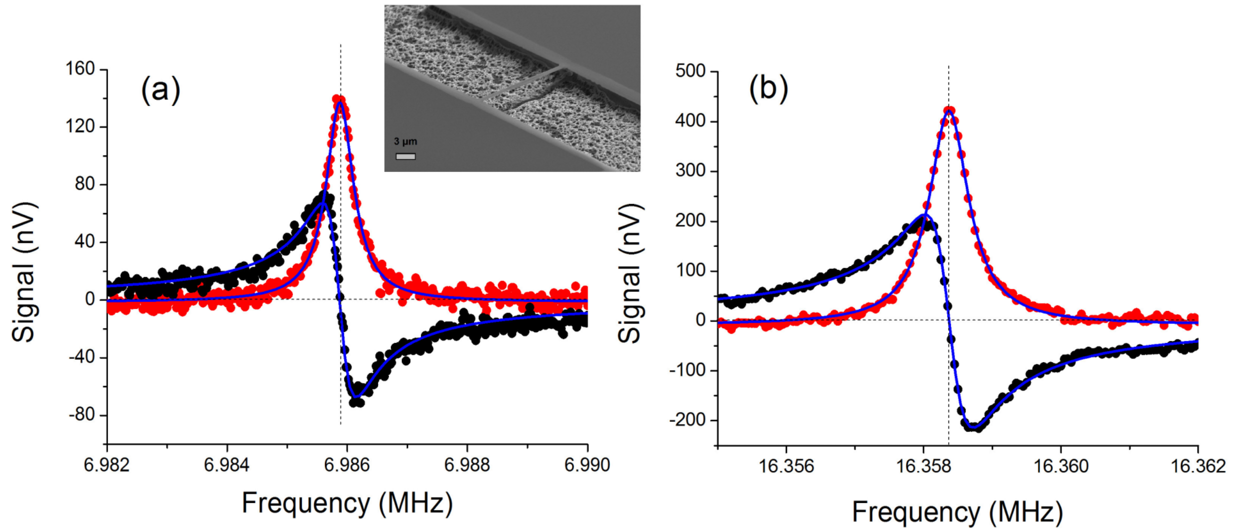

FIG. 2. (Color online) Measurement of the first flexure resonance of two suspended SiN beams with different built-in stresses, where the red points are the in-phase signal and the black points are the out-of-phase signal (both 15 μm long, 250 nm wide, 100 nm thick; see scanning electron microscopy picture in inset). (a) Low-stress and (b) high-stress resonance lines obtained in the linear regime. The lines are Lorentzian fits, with full width at half height of 650 ± 50 Hz (HS, $Q \approx 25\,000$) and 500 ± 50 Hz (LS, $Q \approx 14\,000$). We extract from the resonance frequencies the stress values of 0.85 ± 0.08 GPa (HS) and 0.12 ± 0.05 GPa (LS). Data taken at 4.2 K in vacuum in a 840 mT magnetic field.

The temperature oscillation ($\approx$100 mK) of the membrane is at 2ω and is directly related to its thermal properties by the amplitude and the frequency dependence of the aforementioned temperature oscillation. Since the resistance of the thermometer can be considered as linearly dependent on temperature over that small temperature oscillation, the voltage $V = R[T(2\omega)] \times I(\omega)$ will have an ohmic component at ω and a thermal component at 3ω. By measuring the $V_{3\omega}$ voltage appearing across the transducer as a function of the frequency, both the thermal conductivity and the specific heat of the membrane [22] are inferred. The membranes measured in this study are 300 μm wide and 1.5 mm long.

The transducer of 5 μm width and 1.5 mm length is made out of NbN, whose resistance is strongly temperature dependent. It serves as a thermometer and a heater at the same time [37–39]. For the present work, the thermometer has been designed for the 10 to 320 K temperature range. Typically, the resistance of the thermometer is about 100 kOhm at room temperature with a temperature coefficient of resistance (TCR) $\alpha = \frac{dR}{RdT}$ of 10^{-2} K^{-1} at 300 K and of 0.1 K^{-1} at 4 K.

Since the 1ω voltage is three to four orders of magnitude higher than the 3ω voltage, a specific Wheatstone bridge is used to reduce the 1ω component and perform thermal measurements (see Fig. 3). The bridge consists of the measured sample with a resistance R_e, which is the NbN thermometer on the SiN membrane, the reference thermometer R_{ref} deposited on the bulk region of the chip, which has the same geometry and deposited in the same run as the transducer on the membrane, an adjustable resistor R_v, and an equivalent nonadjustable resistance $R_1 = 50$ kOhm.

The general expression of the measured 3ω output Wheatstone-bridge voltage can be given by [20,21]

$$\left|V_{3\omega}^{\text{rms}}(\omega)\right| = \frac{V_{ac}^{\text{rms}} \alpha Re R_1 |\Delta T_{2\omega}|}{2(R_e + R_1)^2}, \qquad (2)$$

with α the TCR, V_{ac} the 1ω input Wheatstone-bridge voltage, and $|\Delta T_{2\omega}|$ the amplitude of the temperature oscillation at 2ω of the membrane due to the sinusoidal nature of heating.

By solving the partial differential equation of the heat flux across the membrane, Eq. (3) gives the relation between the thermal properties, the dimensions of the membrane, and

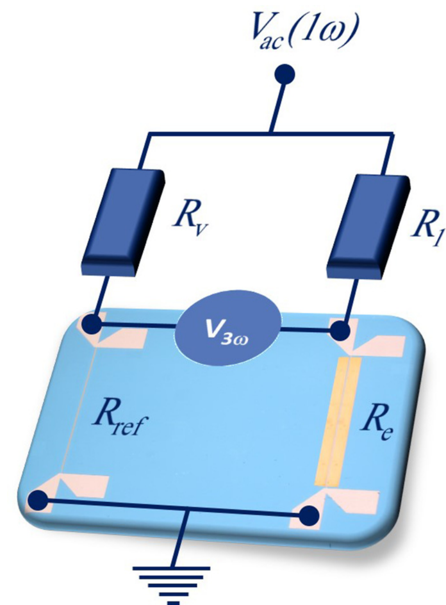

FIG. 3. (Color online) Experimental setup based on the Wheatstone-bridge configuration. The yellow membrane sample is on the bottom right and the reference thermometer is on the left. The blue area of the sketch corresponds to the temperature-regulated part of the Wheatstone bridge.

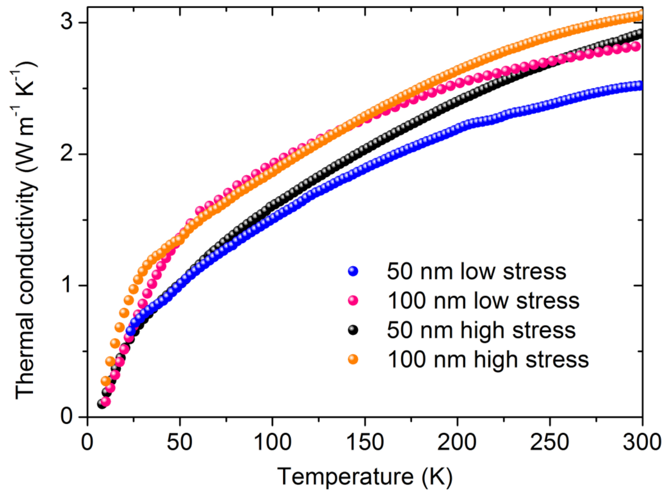

FIG. 4. (Color online) Thermal-conductivity measurement of 50- and 100-nm-thick membranes for both SiN low stress and high stress. The 100 nm curves of low stress and high stress show almost no difference.

$V_{3\omega}$ [20,21]:

$$\left|V_{3\omega}^{\mathrm{rms}}(\omega)\right| = \frac{\alpha\left(V_{ac}^{\mathrm{rms}}\right)^3 R_1 R_e^2}{4K_p(R_e+R_1)^4\left[1+\omega^2\left(4\tau^2+\frac{2\ell^4}{3D^2}+\frac{4\tau\ell^2}{3D}\right)\right]^{1/2}}, \quad (3)$$

with $K_p = \frac{kS}{\ell}$ the thermal conductance and $C = cS\ell$ the heat capacity of the measured membrane, $\tau = \frac{C}{K_p}$ the thermalization time of the membrane to the heat bath, $D = \frac{k}{\rho c}$ the thermal diffusivity, ℓ half the width of the membrane, and S the section of the membrane (perpendicular to the heat flow). By measuring the $V_{3\omega}$ voltage as a function of frequency, both k (in-plane thermal conductivity) and c (specific heat) of the membrane can be extracted [22].

III. EXPERIMENTAL RESULTS

The thermal conductivity of the four different membranes (50 and 100 nm, low stress and high stress) has been measured versus temperature from 10 to 300 K. The experimental data of thermal conductivity are presented in Fig. 4. As expected for amorphous materials, the thermal conductivity of all membranes continuously increases with temperature, as observed by Queen and Hellman [17]. The general trend of the temperature variation of thermal conductivity of all different SiN membranes (LS and HS) is very similar. Only the 50 nm LS membrane seems to have a slightly lower thermal conductivity at room temperature, with a value approaching 2.5 W m^{-1} K^{-1}, instead of 3 W m^{-1} K^{-1} for the others.

In all cases, values of the thermal conductivity at room temperature are approximately 3 W m^{-1} K^{-1}. These values are in accordance with most of the measured in-plane values of thermal conductivity, which are displayed in Table I. Indeed, Jain and Goodson [40] have measured the in-plane thermal conductivity of 1.5-μm-thick SiN specimens to be about 5 W m^{-1} K^{-1}. At the nanoscale, Sultan *et al.* [41] reported thermal conductivity of 500 nm thin films as 3–4 W m^{-1} K^{-1} for a temperature range of 77–325 K. For 180–220-nm-thick LS nitride, Zink and Hellman [16] also observed temperature variation of thermal conductivity ranging from 0.07 to 4 W m^{-1} K^{-1} from 3 to 300 K. The cross-plane thermal conductivity measured by Lee and Cahill [42] for less than 100 nm thickness was in the range of 0.4–0.7 W m^{-1} K^{-1}, showing severely reduced thermal conductivity, which was ascribed to the interfacial thermal resistance. Zhang and Grigoropuolos [43] also observed anomalous thickness dependence and suggested that microstructural defects may strongly influence thermal conductivity. It is important to note that none of the above studies measure thermal conductivity as a function of the internal stress.

In order to verify the coherence of our experimental results, we have extracted the specific heat from the variation of the 3ω signal versus the frequency. Generally, the specific heat is not expected to vary strongly as a function of stress at room temperature [9], and consequently it is a good test for the experiment. The results for the four different membranes are shown in Fig. 5. The temperature variation of the specific heat is very similar for the four samples. For both 50- and 100-nm-thick membranes, we observe that the specific heat tends to be slightly higher for the case of a low-stress sample. But here again, the differences are insignificant and the specific heat is very similar for all of the thicknesses and stress (low and high). The Debye temperatures deduced from the heat-capacity measurements vary from 620 to 650 K depending on the sample, which is a little lower than the commonly accepted value [16]. Our measurements of thermal conductivity and

TABLE I. Measured values of thermal conductivity (k in W m^{-1} K^{-1}) and specific heat (c in J g^{-1} K^{-1}) of silicon nitride having different stoichiometry and/or different stress. Our results are in accordance with most of the studies. LS is for low stress, HS is for high stress, and freest. is for freestanding membranes.

Reference	Deposition	Stoichiometry	Stress	k at 300 K	c at 300 K	Sample
[44]	LPCVD	$Si_{0.66}N_{0.34}$	not measured	3.2	0.7	freest. in plane
[43]	LPCVD	$Si_1N_{1.1}$	not measured	8–10	not measured	freest. out of plane
[40]	LPCVD	Si rich	low stress	4.5	0.5	freest. in plane
[41]	LPCVD	Si rich	low stress	3.5	not measured	freest. in plane
[42]	PECVD-APCVD	$Si_1N_{1.1}$	not measured	0.3	not measured	out of plane
[30]	LPCVD	not measured	high stress	3.2	not measured	freest. in plane
[19]	LPCVD	$Si_1N_{1.1}$	from 0 to 2.4%	2.7 (LS) to 0.4 (HS)	not measured	freest. in plane
This work, LS	LPCVD	$Si_1N_{1.1}$	0.2 GPa	2.5	0.8	freest. in plane
This work, HS	LPCVD	Si_3N_4	0.85 GPa	3	0.8	freest. in plane

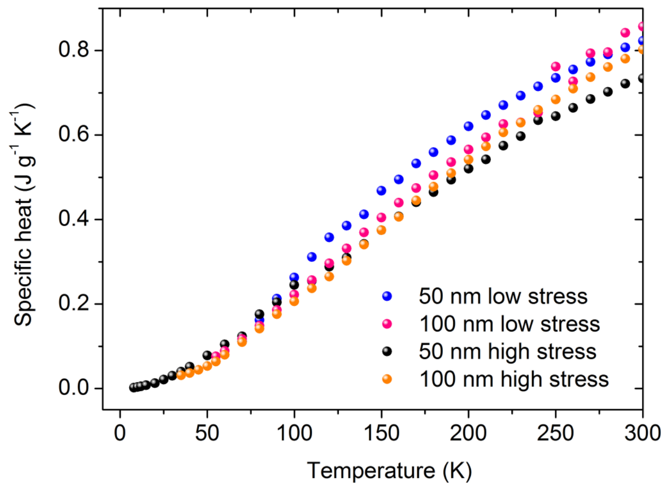

FIG. 5. (Color online) Specific-heat measurement of 50- and 100-nm-thick silicon nitride for both LS and HS, from low temperature (10 K) to room temperature.

specific heat demonstrate that no significant differences occur for the thermal transport in high- and low-stress SiN material because, even with a stress close to 1 GPa, no modification of the phonon thermal conductivity can be observed.

IV. DISCUSSION

High-stress silicon nitride mechanical devices exhibit remarkable Q factors: inverse quality factors Q^{-1} are two to three orders of magnitude lower than those of amorphous SiO_2, from 4 K up to room temperature [2]. The true origin of mechanical dissipation in stressed SiN is still unknown, but could have connections with the thermal properties [2,11,12]. Even though amorphous solids are by nature diverse in composition, these materials are characterized by a universal behavior of the thermal conductivity and mechanical dissipation at low temperature (between 0.1 and 10 K) [45,46]. This universal behavior was initially reported by Zeller and Pohl [46] and described in terms of a phenomenological model which takes into account the contribution from defects, referred to as two-level systems (TLS) [47,48]. The model does reproduce the data, but the universality appears as a surprising coincidence, which continues to puzzle physicists [2,49].

In the theoretical work by Wu and Yu [9], the starting point is to consider that the stress (bond constraints, impurities, local defaults, or even external strain) can modify either the TLS barrier height V or the coupling between TLS and phonons denoted by γ. In this model, it is predicted that the modification of V and γ (by taking into account the amplitude of the stress in stoichiometric SiN) will have a significant effect on the thermal conductivity and mechanical dissipation. Let us discuss the two cases separately. First, when the barrier height is affected, a difference between the thermal conductivity in low and high stress should be seen as the temperature is reduced; a factor close to five at 50 K is expected between the thermal conductivities of LS and HS. This is clearly not observed in our measurements since the thermal conductivity of the HS and LS membranes is very similar. We can only point out that around 50 K, the thermal conductivity is slightly different between the 50 and 100 nm samples, a behavior that can be attributed to a reduction of mean free path in the thinner membrane. Second, in the case of the coupling between phonons and TLS (given by the parameter γ), an effect even larger is expected with a thermal conductivity that is a factor of ten higher in the HS SiN as compared to the LS at room temperature. This could, indeed, be very interesting for practical applications. Even though the stoichiometry is not strictly identical between the low- and high-stress membranes, we do not observe such a big difference in thermal conductivity. This has to be compared to the mechanical measurement performed at 4 K, which also did not present any large differences in mechanical damping between HS and LS devices.

We thus demonstrated the negligible effect of stress on the thermal conductivity and mechanical dissipation in amorphous SiN. We conclude that the hypothesis of TLS in which barrier height V or coupling constant γ is affected by stress does not apply to these materials in the present stress range. We also underline that the values of thermal conductivity we have measured for both high-stress Si_3N_4 and low-stress SiN membranes are in perfect accordance with most of the values already published (see Table I). In order to highlight the low-temperature particularities of the phonon conductivity in these thin membranes, it is particularly important to discuss the temperature variation of the mean free path [18]. Figure 6 shows the phonon mean free path in the membranes determined from the kinetic equation $\Lambda = 3k/Cv_s$, with v_s being the Debye speed of sound. It has been shown by Pohl and co-workers [45] that this equation can be used even at room temperature for amorphous materials. At 300 K, all curves (with the exception of 50 nm LS) approach the same limit, which is two times higher than the interatomic spacing (0.25 nm for amorphous SiN). This is in very good agreement with previous thermal analysis [18]. As the temperature decreases, the mean free path increases rapidly to reach the order of ten nanometers at 20 K. As it can be seen in Fig. 6, it is

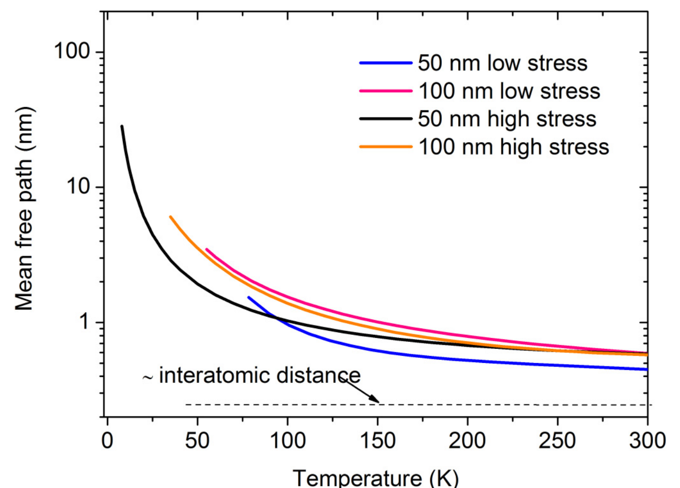

FIG. 6. (Color online) Mean free path Λ of measured samples calculated using experimental data of specific heat and thermal conductivity. The dashed line shows the estimation of the mean free path using the Debye specific heat.

reasonable to ascribe the difference of thermal transport below 200 K to a reduced mean free path in the thinner membranes.

V. CONCLUSIONS

The thermal conductivity has been measured on silicon nitride membranes having low and high stress. The objective was to search for any effect of internal stress on the phonon thermal conductivity and mechanical dissipation. Even though very high stress (of the order of 1 GPa) has been evidenced in suspended stoichiometric SiN membranes by nanomechanical measurements, it has been shown using a very sensitive 3ω technique that the thermal conductivity was not affected. Besides, mechanical dissipation is almost independent of stress, even though high Q's are obtained in HS structures in accordance with the dissipation dilution model. This rules out a scenario of strong increase of thermal conductivity (and concomitantly a strong decrease of mechanical dissipation) with the presence of stress, proposed recently by Wu and Yu [9], either through the increase of the barrier height of two-level systems or through the decrease of the coupling between TLS and phonons. We also show that the thermal properties of the most commonly used silicon nitride materials are equivalent. We then express doubts about the possible use of stress in thermal engineering in amorphous materials.

ACKNOWLEDGMENTS

We acknowledge technical support from Nanofab, the Cryogenic and the Electronic facilities and the Pole Capteur Thermométrique et Calorimétrie of Institut Néel for these experiments. Funding for this project was provided by a grant from La Région Rhône-Alpes (Cible and CMIRA), by the Agence Nationale de la Recherche (ANR) through the project QNM No. 0404 01, and by the European projects: MicroKelvin FP7 low-temperature infrastructure (Grant No. 228464) and MERGING (Grant No. 309150).

[1] S. V. Garimella, Microelectron. J. **37**, 1165 (2006).
[2] D. R. Southworth, R. A. Barton, S. S. Verbridge, B. Ilic, A. D. Fefferman, H. G. Craighead, and J. M. Parpia, Phys. Rev. Lett. **102**, 225503 (2009).
[3] M. Defoort, K. J. Lulla, C. Blanc, O. Bourgeois, E. Collin, and A. D. Armour, Appl. Phys. Lett. **103**, 013104 (2013).
[4] N. Li, J. Ren, L. Wang, G. Zhang, P. Hanggi, and B. Li, Rev. Mod. Phys. **84**, 1045 (2012).
[5] X. Li, K. Maute, M. L. Dunn, and R. Yang, Phys. Rev. B **81**, 245318 (2010).
[6] A. Paul and G. Klimeck, Appl. Phys. Lett. **99**, 083115 (2011).
[7] Y. J. Mii, Y. H. Xie, E. A. Fitzgerald, D. Monroe, F. A. Thiel, B. E. Weir, and L. C. Feldman, Appl. Phys. Lett. **59**, 1611 (1991).
[8] Scott S. Verbridge, Daniel Finkelstein Shapiro, Harold G. Craighead, and Jeevak M. Parpia, Nano Lett. **7**, 1728 (2007).
[9] J. Wu and C. C. Yu, Phys. Rev. B **84**, 174109 (2011).
[10] Y. L. Huang and P. R. Saulson, Rev. Sci. Instrum. **69**, 544 (1998).
[11] Q. P. Unterreithmeier, T. Faust, and J. P. Kotthaus, Phys. Rev. Lett. **105**, 027205 (2010).
[12] P.-L. Yu, T. P. Purdy, and C. A. Regal, Phys. Rev. Lett. **108**, 083603 (2012).
[13] M. M. Leivo and J. P. Pekola, Appl. Phys. Lett. **72**, 1305 (1998).
[14] W. Holmes, J. M. Gildemeister, P. L. Richards, and V. Kotsuboc, Appl. Phys. Lett. **72**, 2250 (1998).
[15] K. Schwab, E. A. Henriksen, J. M. Worlock, and M. L. Roukes, Nature (London) **404**, 974 (2000).
[16] B. L. Zink and F. Hellman, Solid State Commun. **129**, 199 (2004).
[17] D. R. Queen and F. Hellman, Rev. Sci. Instrum. **80**, 063901 (2009).
[18] R. Sultan, A. D. Avery, J. M. Underwood, S. J. Mason, D. Bassett, and B. L. Zink, Phys. Rev. B **87**, 214305 (2013).
[19] M. T. Alam, M. P. Manoharan, M. A. Haque, C. Muratore, and A. Voevodin, J. Micromech. Microeng. **22**, 045001 (2012).
[20] A. Sikora, H. Ftouni, J. Richard, C. Hébert, D. Eon, F. Omnès, and O. Bourgeois, Rev. Sci. Instrum. **83**, 054902 (2012).
[21] A. Sikora, H. Ftouni, J. Richard, C. Hébert, D. Eon, F. Omnès, and O. Bourgeois, Rev. Sci. Instrum. **84**, 029901 (2013).
[22] H. Ftouni, D. Tainoff, J. Richard, K. Lulla, J. Guidi, E. Collin, and O. Bourgeois, Rev. Sci. Instrum. **84**, 094902 (2013).
[23] M. Defoort, K. J. Lulla, C. Blanc, H. Ftouni, O. Bourgeois, and E. Collin, J. Low Temp. Phys. **171**, 731 (2012).
[24] A. N. Cleland and M. L. Roukes, Sensors Actuators A **72**, 256 (1999).
[25] E. Collin, M. Defoort, K. Lulla, T. Moutonet, J.-S. Heron, O. Bourgeois, Yu. M. Bunkov, and H. Godfrin, Rev. Sci. Instrum. **83**, 045005 (2012).
[26] M. Defoort, Non-linear dynamics in nano-electromechanical systems at low temperatures, Ph.D. thesis, Université Joseph Fourier Grenoble, 2014. Typical parameters for our Al-metallized HS mechanical SiN beams are (in first flexure, vacuum at 4.2 K): $f_0 = 0.7$ MHz, $Q_0 = 600\,000$ for 300 μm, $f_0 = 5$ MHz, $Q_0 = 120\,000$ for 50 μm, and $f_0 = 16$ MHz, $Q_0 = 25\,000$ for 15 μm, in good agreement with the literature [35, 36].
[27] M. Defoort (unpublished); see Ref. [26], Sec. II.5.
[28] A. Suhel, B. D. Hauer, T. S. Biswas, K. S. D. Beach, and J. P. Davis, Appl. Phys. Lett. **100**, 173111 (2012)
[29] King Y. Fong, Wolfram H. P. Pernice, and Hong X. Tang, Phys. Rev. B **85**, 161410(R) (2012).
[30] Scott S. Verbridge, Jeevak M. Parpia, Robert B. Reichenbach, Leon M. Bellan, and H. G. Craighead, J. Appl. Phys. **99**, 124304 (2006).
[31] S. Schmid, K. D. Jensen, K. H. Nielsen, and A. Boisen, Phys. Rev. B **84**, 165307 (2011).
[32] K. J. Lulla, M. Defoort, C. Blanc, O. Bourgeois, and E. Collin, Phys. Rev. Lett. **110**, 177206 (2013).
[33] E. Collin, J. Kofler, S. Lakhloufi, S. Pairis, Yu. M. Bunkov, and H. Godfrin, J. Appl. Phys. **107**, 114905 (2010).
[34] A. Olkhovets, S. Evoy, D. W. Carr, J. M. Parpia, and H. G. Craighead, J. Vac. Sci. Technol. B **18**, 3549 (2000).

[35] A. Venkatesan, K. J. Lulla, M. J. Patton, A. D. Armour, C. J. Mellor, and J. R. Owers-Bradley, Phys. Rev. B **81**, 073410 (2010).

[36] T. S. Biswas, A. Suhel, B. D. Hauer, A. Palomino, K. S. D. Beach, and J. P. Davis, Appl. Phys. Lett. **101**, 093105 (2012).

[37] O. Bourgeois, E. André, C. Macovei, and J. Chaussy, Rev. Sci. Instrum. **77**, 126108 (2006).

[38] J. S. Heron, T. Fournier, N. Mingo, and O. Bourgeois, Nano Lett. **9**, 1861 (2009).

[39] A. F. Lopeandia, E. André, J.-L. Garden, D. Givord, and O. Bourgeois, Rev. Sci. Instrum. **81**, 053901 (2010).

[40] A. Jain and K. E. Goodson, J. Heat Transfer **130**, 102402 (2008).

[41] R. Sultan, A. D. Avery, G. Stiehl, and B. L. Zink, J. Appl. Phys. **105**, 043501 (2009).

[42] S. M. Lee and D. G. Cahill, J. Appl. Phys. **81**, 2590 (1997).

[43] X. Zhang and C. P. Grigoropoulos, Rev. Sci. Instrum. **66**, 1115 (1995).

[44] C. H. Mastrangelo, Y. C. Tai, and R. S. Muller, Sensors Actuators **23**, 856 (1990).

[45] R. O. Pohl, X. Liu, and E. Thompson, Rev. Mod. Phys. **74**, 991 (2002).

[46] R. C. Zeller and R. O. Pohl, Phys. Rev. B **4**, 2029 (1971).

[47] W. A. Phillips, J. Low Temp. Phys. **7**, 351 (1972).

[48] P. W. Anderson, B. I. Halperin, and C. M. Varma, Philos. Mag. **25**, 1 (1972).

[49] Dervis C. Vural and Anthony J. Leggett, J. Noncrystal. Solids **357**, 3528 (2011).